XXI IMEKO World Congress "Measurement in Research and Industry"
August 30 - September 4, 2015, Prague, Czech Republic

STATE OF FLOW ESTIMATION IN PNEUMATIC CONVEYING USING ELECTRICAL CAPACITANCE TOMOGRAPHY

M. Neumayer, M. Flatscher, and T. Bretterklieber

Institute of Electrical Measurement and Measurement Signal Processing,
Graz University of Technology, Inffeldgasse 2/II, A-8010 Graz, Austria,
Emai: neumayer@tugraz.at

Abstract **-** Pneumatic conveying has become one of the most favorable transport techniques for bulk solid materials. The metrological assessment of the flow parameters, e.g. mass flow, velocity, as well as the quantification of the flow regime is of crucial interest. However, the nature of the transport system makes measurements challenging. In this work we present an electrical capacitance tomography system for state of flow estimation and demonstrate the abilities of the system by means of test rig measurements.

Keywords: pneumatic conveying, flow measurement, electrical capacitance tomography, inverse problem

1. INTRODUCTION

Granular, or dry bulk material transport systems appear in numerous applications across various fields of industry. Examples can be found in chemical industry, e.g. transport of granular synthetics towards intruders, food industry, e.g. floor transport, or heavy industry, e.g. transport of coal, cement, sand, etc. While granular materials offer favorable properties with respect to some steps of the manufacturing process, e.g. they are easy to portion, the transport process is often affected by this nature in a negative way. Among different transport systems, pneumatic conveying has grown to be the most important transport technique for granular materials [1]. Hereby the granular material is transported by means of a gas stream through an enclosed transport pipe or transport pipe system. Pneumatic conveying is continuously applied to many applications with success. The metrological assessment of the flow properties is still a field of active research. This belongs to the determination of the state of flow itself (flow regime) as well as state variables about the conveying process, e.g. the mass flow, velocity.

The flow regime in pneumatic conveying is of crucial importance for the behavior of the system. Figure 1 illustrates 6 distinct flow regimes with respect to flow velocity an pressure drop for a pneumatic conveying system [1]. Low density flows, which cover the whole diameter of the transport pipe are referred to as dilute flows. They mark one distinct point of operation with respect to pneumatic conveying. For decreased gas velocity and decreased pressure drop a distinct transport layer appears. So called stationary flows or stratified flows are favorable with respect to the energy consumption of the conveying process as the product of pressure drop and velocity is a minimum [1]. A further decrease of the gas velocity results in unstable flow regimes as slug flow. Hereby a plug of accumulated material is immediately moved through the pipe covering most of its cross section. Knowledge about the flow regime is crucial with respect to two points of operation [1]. At first, the energy effort, e.g. the pressure drop times the gas velocity marks the transport losses. Second, the different flow regimes cause different degrees of abrasion with respect to the transport pipes itself. A dilute flow acts like a constant abrasion source while the abrasion due to a slug flow is only temporal. With respect to the term state estimation we refer to state variables as variables, which are related to the energy of the flow. Hereby, the physical parameters of the transport process are of interest, e.g. the mass flow or the gas velocity [2]. Among optical (laser methods, camera), acoustical, electromagnetical (micro wave, x-ray), electrostatic, etc. sensing principles, also capacitive technologies have been investigated [3].

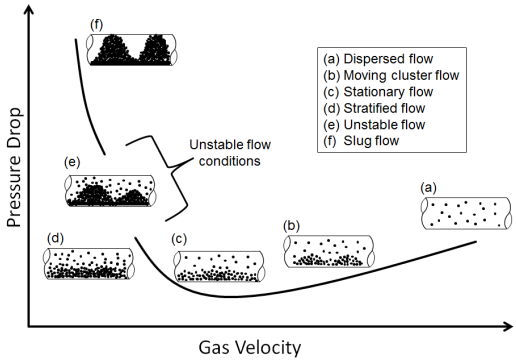

Fig. 1. Categorization of flow schemes as a function of pressure drop over the gas velocity in pneumatic conveying.

In this paper we report on an electrical capacitance tomography (ECT) system for state of flow estimation using the noninvasive measurement technique of ECT [6]. This paper is structured as follows. In section 2 we describe the sensing principle of ECT including the mathematical model development. In section 2 we will discuss the derivation of reconstruction algorithms for real time flow imaging. In section 4 we report first measurement results obtained at a test rig.

2. ELECTRICAL CAPACITANCE TOMOGRAPHY

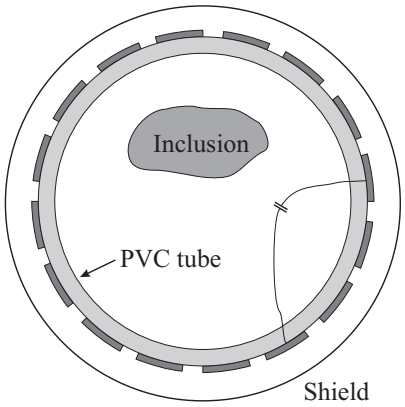

Fig. 2. Scheme of an ECT sensor.

Figure 2 depicts the scheme of an ECT sensor [6]. ECT is a noninvasive measurement technology, which is based on capacitance measurements. In figure 2 one is interested in the material distribution inside the pipe. The distinction between different materials is based on the relative permittivity ε_r. Measurements are taken by means of N_{elec} electrodes, which are mounted on the circumference of the pipe. For N_{elec} electrodes a number of $\frac{N_{\text{elec}}(N_{\text{elec}}-1)}{2}$ independent inter electrode capacitances can be measured between the electrodes. As can be seen, the dielectric material constant is a suitable parameter for ECT, as the permittivity distribution has direct influence on the inter electrode capacitances. The inverse problem of ECT is given by the estimation of the permittivity distribution from measurements.

2.1. Measurement Process and Sensor Simulation

Sensor modeling refers to the process of deriving a mathematical description for a measurement process $P : \phi \mapsto \tilde{\boldsymbol{d}}$. Hereby, $\tilde{\boldsymbol{d}} \in \mathbb{R}^M$ are the measurements, which are the output of the measurement process $\tilde{\boldsymbol{d}} = P(\phi)$. The measurement process provides the relation between the quantity of interest ϕ and the data $\tilde{\boldsymbol{d}}$. Sensor simulation is the task of solving the equations of the mathematical sensor model. We refer to the simulation process as forward map $F : \boldsymbol{x} \mapsto \boldsymbol{y}$, where $\boldsymbol{x}$ is the simulation input and $\boldsymbol{y}$ is the simulation output. For many problems the vector $\boldsymbol{x} \in \mathbb{R}^N$ is obtained from ϕ by means of a discretization $D : \phi \mapsto \boldsymbol{x}$. The discretization D is designed with respect to the representation of ϕ, but can also be influenced by the (numerical) simulation technique used within the forward map. E.g. for the simulation of the ECT sensor we use a finite element (FE) approach. Then a natural choice for D is given by the finite elements itself.

The measurement process of ECT is governed by the Maxwells equations [6]. For the measurements, an AC voltage is applied to one electrode while the potentials of all other electrodes are fixed to GND potential, e.g. by means of a transimpedance amplifier to measure the displacement current from the active electrode. As the current is proportional to the capacitance between two electrodes, it can be used to measure the inter electrode-capacitances. This process is consecutively performed for each of the N_{elec} electrodes. Due to the used measurement frequencies and the vastly absence of conductive materials (otherwise ECT is not the favorable measurement system), the measurement process can be approximated by means of the electrostatic case. Thus, the potential equation $\nabla \cdot (\varepsilon_0 \varepsilon_r \nabla V) = 0$ is used to describe the sensor effects in a domain Ω. V is the electric scalar potential and ε_0 and ε_r are the absolute and the relative permittivity, respectively. With respect to figure 2 the domain Ω is given by the interior of the pipe, the pipe itself and the outer space, which is bounded by the shield. The measurement process is modeled by means of Dirichlet type boundary conditions, e.g. $V_{\Gamma_j} = V_0$ is applied on the surface Γ_j of the active electrode and $V_{\Gamma_i} = 0$ for $i \neq j$ on the remaining electrodes. Further we apply $V_{\partial\Omega} = 0$ for the screen, which is the boundary $\partial\Omega$ of the domain Ω. Then the inter electrode capacitances are given by Gauss law

$$c_{i,j} = \frac{1}{V_0} \int_{\Gamma_i} \vec{n} \cdot \varepsilon_0 \varepsilon_r \nabla V_j ds, \tag{1}$$

where V_j is the potential distribution for the j^{th} electrode being active. By means of the FE method for sensor simulation, this procedure results in a FE equation system of form $\boldsymbol{K}(\boldsymbol{x})\boldsymbol{V} = \boldsymbol{R}$, where $\boldsymbol{K}(\boldsymbol{x})$ is a FE stiffness matrix, $\boldsymbol{V}$ is a matrix whose N_{elec} column vectors are the discrete solution vectors and $\boldsymbol{R}$ holds the N_{elec} right hand side vectors. For the capacitance computation a discrete version of (1) can be assembled, e.g. the capacitance matrix $\boldsymbol{C} = [c_{i,j}]$ can be computed by means of a matrix matrix product $\boldsymbol{C} = \boldsymbol{M}\boldsymbol{V}$, where $\boldsymbol{M}$ is referred to as measurement matrix.

3. ECT RECONSTRUCTION

In this section we will point out the derivation of reconstruction algorithms to estimate $\boldsymbol{x}$ from data $\tilde{\boldsymbol{d}}$. Due to its versatility, we will derive this algorithms using Bayes law [4], [5].

$$\pi(\boldsymbol{x}|\tilde{\boldsymbol{d}}) \propto \pi(\tilde{\boldsymbol{d}}|\boldsymbol{x})\pi(\boldsymbol{x}). \tag{2}$$

Hereby, $\pi(\tilde{\boldsymbol{d}}|\boldsymbol{x})$ is the likelihood function and $\pi(\boldsymbol{x})$ is the prior. Both terms are probability density functions (pdf). The likelihood function provides a probability measure for $\boldsymbol{x}$ having caused the data $\tilde{\boldsymbol{d}}$. Thus, the likelihood relates the model F, the data $\tilde{\boldsymbol{d}}$ and the disturbance of the measurements due to noise. E.g. for zero mean additive Gaussian noise the likelihood function is given as a multivariate Gaussian distribution $\pi(\tilde{\boldsymbol{d}}|\boldsymbol{x}) = \mathcal{N}(y(\boldsymbol{x}) - \tilde{\boldsymbol{d}}, \boldsymbol{\Sigma}_v)$, where $\boldsymbol{\Sigma}_v$ is the covariance matrix of the noise. The prior distribution is a pdf, which can be designed to incorporate any knowledge about $\pi(\boldsymbol{x})$. The application of a prior distribution is essential for the stable solution of inverse problems due to their ill-posed nature [5]. A generic prior, which is

often used for ECT is given by $\pi(x) \propto \alpha \boldsymbol{x}^T \boldsymbol{L}^T \boldsymbol{L} \boldsymbol{x}$ [6], where $\boldsymbol{L}$ can be designed to enforce certain solutions, e.g. smooth solutions. The posterior distribution $\pi(\boldsymbol{x}|\tilde{\boldsymbol{d}})$ in equation (2) provides a probability measure for $\boldsymbol{x}$ being the solution given the data $\tilde{\boldsymbol{d}}$ and the model. The advantage of the Bayesian framework is given by the possibility to incorporation any knowledge (model, noise, prior, etc.) [5].

An important point estimator, which can be derived from the Bayesian framework is the maximum a posteriori estimator (MAP). For the stated likelihood and the generic prior, the MAP estimator is given by [4]

$$\boldsymbol{x}_{\mathrm{MAP}} = \arg\min_{\boldsymbol{x}} ||\boldsymbol{C}\left(\boldsymbol{y}(\boldsymbol{x}) - \tilde{\boldsymbol{d}}\right)||_2^2 + \alpha \boldsymbol{x}^T \boldsymbol{L}^T \boldsymbol{L} \boldsymbol{x}. \quad (3)$$

The matrix $\boldsymbol{C}$ can be obtained from the Cholesky decomposition of the precision matrix, which is the inverse of the covariance matrix Σ_v. Due to the nature of the forward map, the computation of the MAP estimate results in a nonlinear optimization problem of Gauss-Newton type. A solution can be found iteratively by solving

$$\begin{aligned} \boldsymbol{x}_{k+1} &= \boldsymbol{x}_k - s\left(\boldsymbol{J}_k^T {\boldsymbol{\Sigma}_{\boldsymbol{v}}}^{-1} \boldsymbol{J}_k + \alpha \boldsymbol{L}^T \boldsymbol{L}\right)^{-1} \cdot \\ &\quad \left(\boldsymbol{J}_k^T {\boldsymbol{\Sigma}_{\boldsymbol{v}}}^{-1} (\boldsymbol{y}(\boldsymbol{x}_k) - \tilde{\boldsymbol{d}}) + \alpha \boldsymbol{L}^T \boldsymbol{L} \boldsymbol{x}_k\right) \quad (4) \end{aligned}$$

where $\boldsymbol{J}$ is the Jacobian of the forward map F and s is a step-width parameter. However, an iterative reconstruction is not suitable for online state of flow estimation, as the computational effort is to high. Instead only one step of the iteration scheme is used leading to

$$\begin{aligned} \boldsymbol{x} &= \boldsymbol{x}_0 - \left(\boldsymbol{J}_0^T {\boldsymbol{\Sigma}_{\boldsymbol{v}}}^{-1} \boldsymbol{J}_0 + \alpha \boldsymbol{L}^T \boldsymbol{L}\right)^{-1} \cdot \\ &\quad \boldsymbol{J}_0^T {\boldsymbol{\Sigma}_{\boldsymbol{v}}}^{-1} (\boldsymbol{y}(\boldsymbol{x}_0) - \tilde{\boldsymbol{d}}). \quad (5) \end{aligned}$$

As can be seen, the reconstruction result can be obtained by a single matrix vector multiplication, e.g.

$$\boldsymbol{x} = \boldsymbol{x}_0 - \boldsymbol{F}_{\mathrm{r}} (\boldsymbol{y}(\boldsymbol{x}_0) - \tilde{\boldsymbol{d}}), \quad (6)$$

where $\boldsymbol{F}_{\mathrm{r}} = \left(\boldsymbol{J}_0^T {\boldsymbol{\Sigma}_{\boldsymbol{v}}}^{-1} \boldsymbol{J}_0 + \alpha \boldsymbol{L}^T \boldsymbol{L}\right)^{-1} \boldsymbol{J}_0^T {\boldsymbol{\Sigma}_{\boldsymbol{v}}}^{-1}$ holds. This linear reconstruction is suitable for online state of flow estimation. As $\boldsymbol{F}_{\mathrm{r}}$ is built from a local linearization, the reconstruction can only be considered suitable for small deviations of $\boldsymbol{x}$. However, this holds for the typical materials and the conveying conditions in pneumatic conveying.

There are also alternative methods to create a reconstruction matrix $\boldsymbol{F}_{\mathrm{r}}$, e.g. the so called optimal first and second order approximations (OFOA, OSOA) can be used to create a matrix $\boldsymbol{F}_{\mathrm{r}}$ using a sampling scheme [6].

4. RESULTS AT TEST RIG

In this section we want to present first results for state of flow estimation using an ECT sensor. Figure 3 depicts a our sensor setup. The electrodes of the ECT sensor are fabricated by means of copper tape, which are placed on a sheet of paper. The paper is wrapped around the process pipe. For the ECT measurements a low-Z carrier principle [7] is used, which directly measures the displacement current as discussed in the modeling section. A remarkable fact of the lab sensor system is given by the number of electrodes, which is only 5. Thus, only 10 independent measurements can be obtained.

As can be seen, the electrodes are completely exposed to the outer environment due to the absence of a screen. We do not recommend such a system for an industrial use, yet under lab conditions it can be used to provide sufficient results. Before performing reconstruction experiments, two calibration measurements were performed. Using an empty measurement and a measurement with a defined filling of the pipe, a linear transform of the measurement readings is created, to match the model output to the corresponding measurement readings. This step compensates offset and gain differences of the electronics.

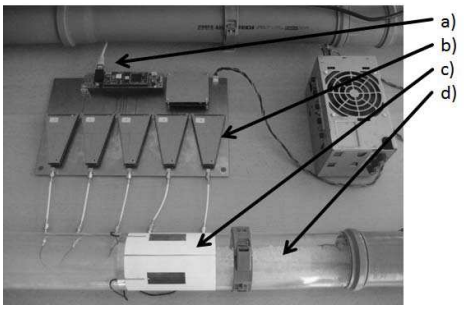

Fig. 3. Lab setup for flow imaging in pneumatic conveying using a reduced ECT sensor. Components: a) Data connection to host PC, b) Measurement electronics, c) Electrodes of the reduced ECT sensor, d) Pipe of pneumatic conveying process.

Figure 4 provides a close view on the pipe and the sensor section for one flow experiment. For this experiment a slug flow has been created. The pipe was first filled with plastic particles. For our test rig an air blower is used to create a constant air stream to create dilute flows. In combination with a nozzle to inject compressed air, rapid material movements can be created. As can be seen in figure 4, the plug offers a linear grow at its front and has a sharp cutoff at its end, where it is pushed by the air provided by the nozzle.

Figure 5 depicts a series of reconstruction results. As can be seen, the time series of the reconstruction results illustrates the plug. For the reconstruction a linearized algorithm as discussed in section 3 has been used. In our model the interior of the pipe was discretized using ≈ 650 elements, which gives the dimension of the state vector $\boldsymbol{x} \in \mathrm{R}^N$ to be estimated from the 10 independent measurements. As can be seen, the reconstruction results covering the center of the plug offer some artefacts, e.g. a denser part. This is

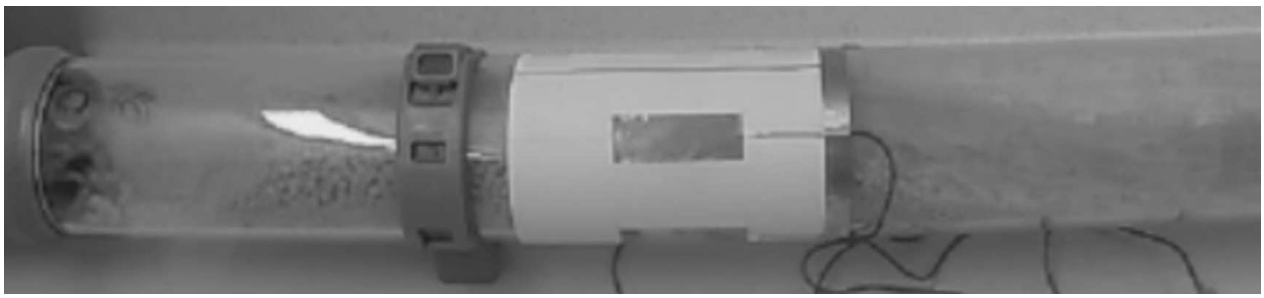

Fig. 4. Photography of a flow experiment. The pipe section in upstream direction of the sensor was completely filled with plastic particles. An air blower and a compressed air nozzle are used to push a material plug in downstream direction.

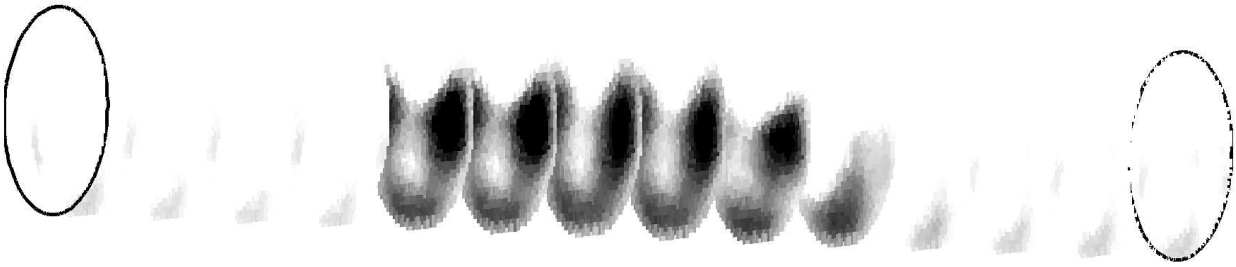

Fig. 5. Reconstruction results for the slug flow experiment depicted in figure 4. The geometry of the plug is clearly visible. Note, that the graphic was created without an exact length scaling with respect to the sensor geometry.

due to the low number of electrodes. Typical ECT systems maintain at least 8 electrodes. However, the system can already be used to provide a suitable measure for the void fraction. In combination with a velocity measurement the mass flow can be estimated. Also the flow regime can be clearly identified.

5. CONCLUSION AND OUTLOOK

In this work we presented the possibility of state of flow measurement by means of electrical capacitance tomography. We discussed the principle of ECT and the deviation of reconstruction algorithms. We used the Bayesian framework as a general framework to incorporate any available knowledge. In section 4 we demonstrated the ability for state of flow reconstruction using a sensor with 5 electrodes only. The final paper will include a more detailed description of some specifics, as well as an extension for velocity measurements using a twin plane ECT system and comparative measurements.

REFERENCES

[1] G.A. Jama, G.E. Klinzing, and F. Rizk. *An Investigation of the Prevailing Flow Patterns and Pressure Fluctuation Near the Pressure Minimum and Unstable Conveying Zone of Pneumatic Transport System*. Powder Technology,112:87-93, 2000.

[2] Y. Yan. *Mass flow measurement of bulk solids in pneumatic pipelines*, Measurement Science and Technology, vol. 7, pp. 1687 - 1706, 1996.

[3] Y. Zheng and Q. Liu. *Review of techniques for the mass flow rate measurement of pneumatically conveyed solids*. Measurements, vol. 44, pp. 589 - 604, 2011.

[4] D. Watzenig and C. Fox, *A review of statistical modelling and inference for electrical capacitance tomography*, Measurement Science and Technology, vol. 20, no. 5, 2009.

[5] J. P. Kaipio and E. Somersalo, *Statistical and computational inverse problems*, Springer New York: Applied Mathematical Sciences, 2004.

[6] M. Neumayer, H. Zangl, D. Watzenig, and A. Fuchs, *Current reconstruction algorithms in Electrical Capacitance Tomography*. New Developments and Applications in Sensing Technology, Springer, 2011.

[7] H. Wegleiter, A. Fuchs, G. Holler, and B. Kortschak. *Development of a displacement current-based sensor for electrical capacitance tomography applications*. Flow Measurement and Instrumentation, vol. 19, no. 5, pp. 241 250, 2008. [Online].